

Adsorption of Polyamides and the Stability of Dispersion

TATSUO SATO, *Sony Corporation Research Center, Tokyo, Japan*

Synopsis

The stability of red iron oxide, titanium dioxide, and carbon black dispersed in cyclohexanone and isopropyl alcohol solutions of fatty polyamides was studied by measuring adsorption, viscosity, zeta potential, and sedimentation volumes. It was found that the stability of dispersion is markedly affected by the adsorption of polyamides. The greater the amount of adsorption, the greater the stability. On the other hand, a negative adsorption impaired the stability. A stabilization mechanism of polyamide adsorption was discussed in terms of entropic repulsion, electrostatic repulsion, and van der Waal's attraction.

INTRODUCTION

The stabilization of dispersion may occur by either double-layer electrostatic repulsion or by entropic repulsion of the interacting adsorbed molecules. The increase in the repulsion potential prevents their mutual approach to within a distance where van der Waal's attraction energy would overcome their thermal motion. The theoretical treatment on the relationship between electrical charge and stability of dispersion in aqueous media has been well established by Verwey and Overbeek¹ and developed by Koelmans and Overbeek² to nonaqueous media, investigators who have satisfactorily accounted for many experimental facts. The theoretical approach to the mechanism of entropic repulsion was reported by several workers.³⁻⁷ Little work, however, has been published on the application of these theories to the practical systems,⁸⁻¹⁰ probably because of the difficulties in determining the dimensions of complex configurations of adsorbed polymer molecules.

This work was made with the purpose of investigating the effects of electrical repulsion and entropic repulsion on the stability of dispersion in polymer solutions by determining the adsorption of polymer and zeta-potentials. An attempt was made to calculate the potential energies of the colliding particles based on some assumptions.

Polymers used were fatty polyamides of various molecular weights and amine values, which are well known to exhibit a remarkable surface-active property at the solid-liquid interface in nonaqueous solutions.¹¹⁻¹³

EXPERIMENTAL

Materials

Fatty polyamides of various molecular weights and amine values were obtained from General Mills Co., Ltd. A typical example of these structures is



where R is an aliphatic carbon group containing 34 carbon atoms.

The amine values were determined by titration with diluted hydrochloric acid using bromocresol green as an indicator. The amine value is expressed as the number of milligrams of KOH equivalent to the base content of 1 g of fatty polyamide. The approximate molecular weights, viscosities, and specific gravities supplied from the manufacture are shown in Table I together with the weight-average molecular weight distributions determined by gel permeation chromatography. The conditions of measurements were: combination of column: 10^7 , 10^6 , 10^5 , 10^4 , and 10^3 ; solvent: tetrahydrofuran; polymer concentration: 2 wt-%.

The lowest molecular weight of polyamides given in Table I is slightly smaller than the calculated value from the molecular structure with substituting 1 for n . This is attributed to the presence of small quantities of polyamides whose aliphatic chains are shorter than 34 carbon atoms which are brought from the reactant, dibasic acid having the shorter aliphatic chain.

TABLE I
Properties of Polyamides

Poly-amides	Mol. wt.	Mol. wt. distribution (M_w/M_n) ^a	Amine value	Viscosity, poises	Specific viscosity at 25°C
A	3,000	4.14	93.1	8-11 at 150°C	0.97
B	1,400	2.91	227.8	32-36 at 75°C	0.97
C	900	2.18	288.4	7-9 at 75°C	0.97
D	700	1.89	353.4	4 at 75°C	0.97
E	500	1.60	350.1	7 at 25°C	0.95

^a M_w : Weight-average molecular weight; M_n : number-average molecular weight.

Solvents used were reagent-grade cyclohexanone and isopropyl alcohol. Their properties are listed in Table II.

TABLE II
Properties of Solvents

Solvent	Dielectric constant	Viscosity	Solubility parameter
Cyclohexanone	18.3 (20°C)	2.45 (15°C)	9.88
Isopropyl alcohol	18.6 (20°C)	2.41 (20°C)	11.30

Adsorbents used were red iron oxide ($\alpha\text{-Fe}_2\text{O}_3$), anatase titanium dioxide (TiO_2), and carbon black, the properties of which are listed in Table III. Surface areas were determined by the BET method using nitrogen at 77°K, taking a value of $16.2 \times 10^{-16} \text{ cm}^2$ for the area of an adsorbed nitrogen molecule. Mean particle diameters were obtained from size analysis by electron microscopy.

TABLE III
Properties of Pigments

Pigment	Supplier	Mean particle diameter, μ	Surface area, m^2/g
Titanium dioxide (anatase)	Ishihara Sangyo	0.15-0.25	7.85
Carbon black	Columbia Carbon		691.00
Red iron oxide	Sony	{ long axis 0.16-0.20 short axis 0.10	8.38

Procedures

Determination of Adsorption

Carefully stoppered glass bottles containing known amounts of adsorbent and polymer solution were agitated gently at room temperature overnight. The supernatant solution was then centrifuged and analyzed for polymer concentration. Polyamide concentration was determined by a titration with diluted hydrochloric acid for the amine groups. The amount of adsorption was calculated from the change in polymer concentration in the supernatant liquid. The effect of acid or alkaline impurities which may be contained in the adsorbents was correlated, although the effect was almost negligible.

Electrophoresis Measurement

A microelectrophoretic method was employed since this method, according to Kitahara,¹⁴ gives the most correct values for the determination of zeta potential of nonaqueous dispersions. The suspensions were diluted further with the corresponding polyamide solutions to facilitate vision in the electrophoretic path. The field of 25 V/cm was applied after confirming that there is a linear relationship between the applied potentials and electrophoretic mobilities in the range 15-25 V/cm. The viscosities of the solutions were determined by an Ubbelohde viscometer at 25°C. Zeta potentials, ζ , were calculated using Hückel's equation which is applicable to systems for which the thickness of the double layer is large compared with the radius of the particle,

$$\zeta = \frac{6\pi\eta u}{\epsilon} \quad (1)$$

where η and ϵ are the viscosity and dielectric constant of the medium, respectively, and u is the electrophoretic mobility.

Determination of the Thickness of Adsorbed Layer

The thickness of the adsorbed layer was calculated from the determination of the viscosity of suspension using the Guth-Gold equation¹⁵ which was derived by modifying the classical Einstein equation:

$$\eta = \eta_0(1 + 0.67f\phi + 1.62f^2\phi^2 + \dots) \quad (2)$$

where η is the viscosity of suspension, η_0 is the viscosity of medium, ϕ is the apparent volume fraction of the dispersed phase, and f is the shape factor (=length/breadth). The f value was obtained directly from electron-microscopic determination. The average value of f was 1.8, with a standard deviation, σ , of 0.20, for ten particles of red iron oxide. The average thickness of the adsorbed layer was obtained by dividing the difference between the apparent and actual dispersed phase volume by the surface area of the dispersed particles, assuming that the polymer was adsorbed over the whole of the available surface of adsorbent. The errors of the thickness due to the deviation of f were less than 20%.

Care should be taken in the application of this method when particles are flocculated. A very large thickness is obtained under the presence of flocculation, since the immobilized solvent molecules captured in the space of the flocculants give a very large apparent volume fraction of dispersed phase.¹⁶⁻¹⁸ Therefore, the thickness was calculated only for the systems in which the particles are completely deflocculated.

Determination of Stability of Dispersion

The stability of the dispersion was determined by a sedimentation method. The pigments were dispersed by ball-milling in the polymer solutions in glass bottles overnight (more than 15 hr). The solution was then poured into a sedimentation test tube, and the sedimentation rate and the sedimentation volume were measured. The evaluation of the stability was graded 1 (very unstable) to 5 (very stable).

RESULTS AND DISCUSSION

Adsorption Isotherm

The adsorption isotherms of polyamide A and D on red iron oxide from cyclohexanone solution are shown in Figure 1. These curves are similar in shape to a Langmuir isotherm, giving linear plots of CA^{-1} against C , as shown in Figure 2, where C is the concentration of polyamide and A is the amount of adsorption. It is interesting to note that, although the slopes of the curves decrease with increasing polyamide concentration, they do not reach a plateau even at such high concentrations as 8 g/dl. This may be attributed to the fairly low molecular weights of the polyamides¹⁶ and to the complexity of configurations of adsorbed polyamides molecules.

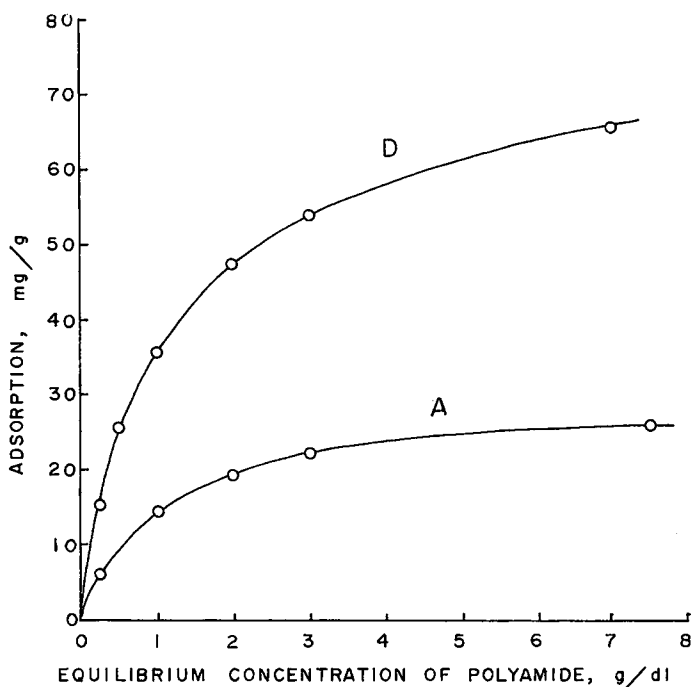


Fig. 1. Adsorption isotherms of polyamides A and D on red iron oxide from cyclohexanone at 4 g/dl pigment concentration.

Effect of Amine Values

The amount of adsorption of polyamides from cyclohexanone increased with increase in the amine value of polyamides, as shown in Figure 3, indicating that polyamide molecules are adsorbed by attaching the polar amine groups onto the polar adsorbent surface as the anchor segments. Wittcoff¹³ reported from a calorimetric measurement that the heat of adsorption of polyamide onto metal oxide per amine equivalent is higher than that of the physical adsorption, indicating the amine group adsorbs very strongly onto metal oxide, presumably by chemisorption. Although the effect of carboxyl groups on the adsorption is not evident in this study, it seems to be much smaller than that of amine groups. It is of interest to note that it is unlikely that the adsorption is dependent on the molecular weights. According to Perkel and Ullman,¹⁹ assuming that the amount of adsorption is independent of the molecular weight, the possible model is one where all segments of the polymer molecule lie in the plane of the adsorbent.

Effect of Concentration and Polarity of Adsorbent

The amount of adsorption of polyamide A from cyclohexanone solution onto unit surfaces of adsorbents against adsorbent concentration is shown in Figure 4. The amount of adsorption on unit surfaces of titanium dioxide

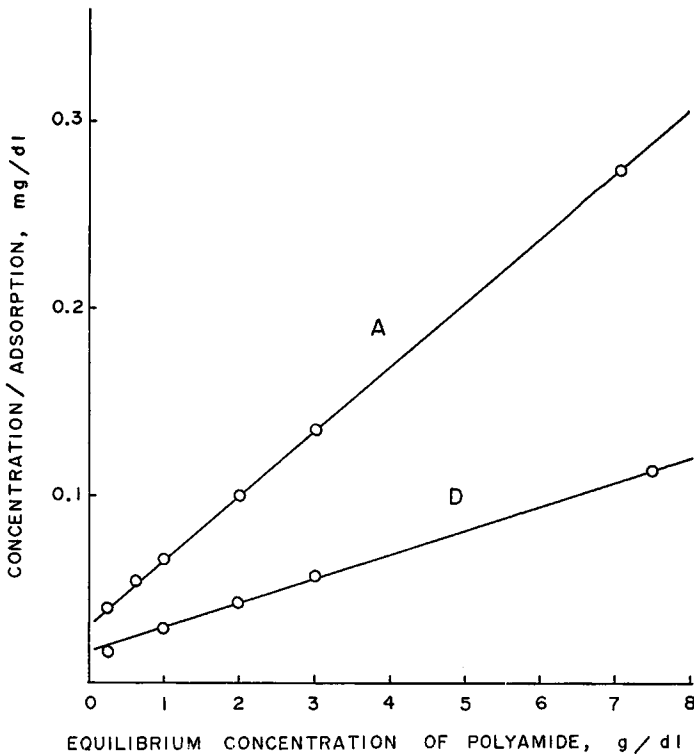


Fig. 2. Langmuir plots of polyamides A and D.

and red iron oxide decreases markedly with increasing adsorbent concentration, whereas that on carbon black does not. This indicates that the available surfaces per unit amount of titanium dioxide and red iron oxide decrease with increasing concentration due to flocculation. In order to obtain the amount of adsorption in an ideal state that is, in the absence of particle-particle interaction, one should extrapolate the curve to zero adsorbent concentration.

To study the effect of polarity of adsorbents, carbon black was used as nonpolar (or very weakly polar) adsorbent and red iron oxide and titanium dioxide, as polar ones. Figure 4 shows that red iron oxide and titanium dioxide adsorb polyamides markedly, while carbon black does not. This fact is more evidence that the amine groups contribute to the adsorption.

Effect of Solvent

Two main effects may be discerned, i.e., solvent power and the competition of adsorption between solvent molecule and polymer molecule. According to many investigators,²⁰⁻²⁵ the amount adsorbed from a solution is largest when a poor solvent for the polymer is used and decreases progressively with increase in solvent power.

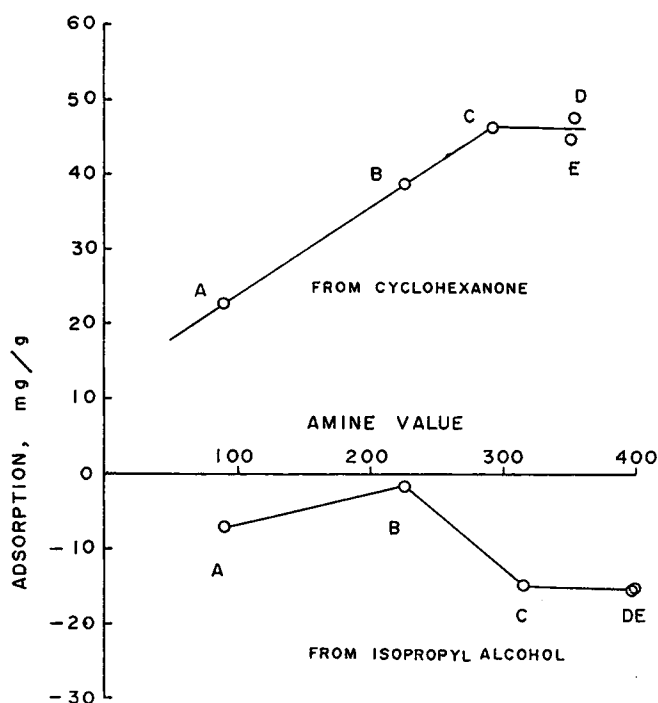


Fig. 3. Adsorption of polyamides A, B, C, D, and E on red iron oxide from cyclohexanone and isopropyl alcohol vs. amine values of polyamides.

The rating of solvent power may be made in terms of intrinsic viscosity, $[\eta]$, good solvents causing expansion of the dissolved chain and so giving high intrinsic viscosities. The intrinsic viscosities of polyamides measured by an Ubbelohde viscometer at 25°C are shown in Table IV, which indicates that cyclohexanone is a better solvent for polyamides than is isopropyl alcohol.

TABLE IV
Intrinsic Viscosities

Polyamide	Solvent	$[\eta]^{25^\circ\text{C}}$, dl/g
A	cyclohexanone	0.109
A	isopropyl alcohol	0.096
C	cyclohexanone	0.071
C	isopropyl alcohol	0.064
E	cyclohexanone	0.042
E	isopropyl alcohol	0.033

The amounts of adsorption onto red iron oxide from two solvents are shown in Figure 3. Polyamides are adsorbed markedly from cyclohexanone, while they are negatively adsorbed from isopropyl alcohol. This result is contrary to the former reports described above. An explanation of this can

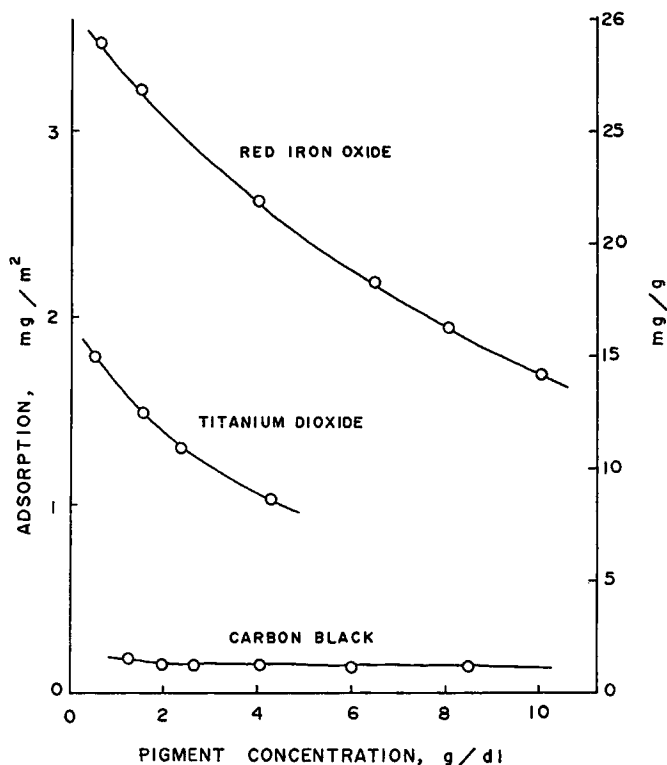


Fig. 4. Adsorption of polyamide A on unit surface of adsorbents from cyclohexanone at 3 g/dl polyamide concentration vs. pigment concentration.

be found in the interaction between solvent and adsorbent, for the wettability of cyclohexanone on polar adsorbent is smaller than that of isopropyl alcohol, which was verified by a sedimentation test. Consequently, in this system, the contribution of the effect of competition of adsorption is greater than that of solvent power. The negative adsorption occurred because isopropyl alcohol molecules adsorb preferentially, resulting in an increase in polyamide concentration of the bulk of the solution.

Effect of Moisture

Red iron oxide has dried for 3 and 7 hr at -690 mm Hg and 80°C , and the adsorption onto the red iron oxide thus dried was compared with that of nondried red iron oxide. The result in Figure 5 shows that the adsorption of polyamide is insensitive to atmospheric moisture.

Thickness of Adsorbed Layer

The apparent volume fraction, ϕ , and the thickness of adsorbed layers determined from the viscosity measurements of suspensions are shown in Table V, together with the thickness of adsorbed layers calculated directly

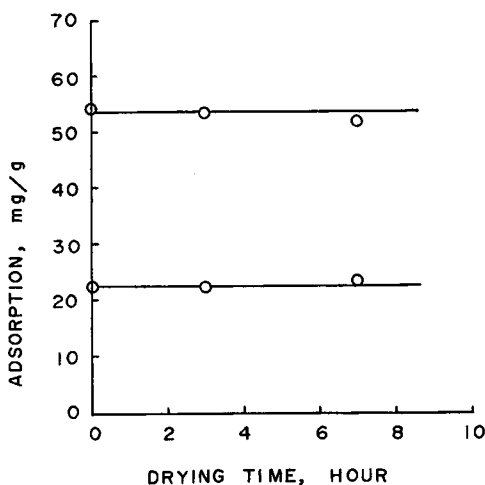


Fig. 5. Adsorption of polyamide A and D on red iron oxide from cyclohexanone vs. time for drying adsorbent.

from the amount of adsorption, assuming that polyamides are adsorbed in a closely packed layer. Calculations of the thickness from the apparent volume fractions were made only for the systems in which the particles are considered to be completely deflocculated because of the reasons described in the preceding section. The thickness calculated from the viscosity measurements were smaller than those calculated directly from the amounts of adsorption. This is probably due to the difference between dynamic and static measurements. It appears that the lyophilic aliphatic chains extending into the bulk of solutions do not contribute to the increase in dynamic

TABLE V
Thickness of Adsorbed Layers on Red Iron Oxide

Polyamide concentration, g/dl	Solvent	Polyamide	$\eta_{\gamma}^{25^{\circ}\text{C}}$	ϕ	Thickness	
					Calculated from ϕ	Calculated from A_i
3	cyclohexanone	A	1.022	0.018	16	21
3	cyclohexanone	B	1.025	0.021	20	36
3	cyclohexanone	C	1.025	0.021	20	—
3	cyclohexanone	D	1.026	0.022	24	40
3	cyclohexanone	E	1.037	0.031	—	40
3	isopropyl alcohol	A	1.037	0.031	—	—
3	isopropyl alcohol	D	1.040	0.033	—	—
3	isopropyl alcohol	E	1.037	0.031	—	—
10	cyclohexanone	A	1.028	0.022	24	34
10	cyclohexanone	B	1.038	0.031	35	—
10	cyclohexanone	C	1.038	0.031	35	—
10	cyclohexanone	D	1.038	0.031	35	99
10	cyclohexanone	E	1.044	0.035	—	99

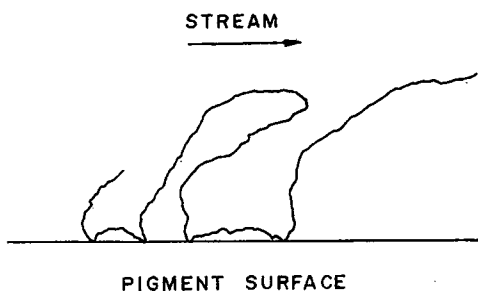


Fig. 6. Deformation of adsorbed polyamide molecules by stream of solution.

viscosity, since they will be easily deformed by the stream of solution in the capillary of the viscometer, as illustrated in Figure 6.

Effect of Adsorption on Dispersion

The stabilities of dispersions of red iron oxide in 3 g/dl polyamide solutions determined from sedimentation tests are shown in Table VI. By comparison with the results of the adsorption of polyamides, it will be found that there is a close relationship between adsorption and stability of dispersions. The greater adsorption of polyamides results in greater stability of dispersion, while negative adsorption impairs stability.

TABLE VI
Dispersion Stabilities of Red Iron Oxide in Polyamide Solutions at Polyamide Concentration of 3 g/dl and pigment concentration of 10 g/dl

Solvent	Polyamide	Time needed to centrifuge, min	Sedimentation volume, ml	Evaluation
Cyclohexanone	A	30	9.5	3
	B	90	3.6	5
	C	90	3.3	5
	D	90	3.2	5
	E	15	8.5	3
	none	15	12.8	2
Isopropyl alcohol	A	60	11.0	3
	B	30	11.1	2
	C	15	13.3	1
	D	15	13.0	1
	E	15	13.1	1
	none	60	11.1	3

An attempt was made here to discuss the significance of entropic repulsion of the adsorbed layer in terms of potential energy. Since it seems to be almost impossible to obtain absolute values for potential energy, relative values were calculated based on some assumptions to compare the height of potential energy with that of electrostatic repulsion.

The entropic repulsion potential energy of adsorbed polyamide molecules was calculated from Mackor's equation. According to Mackor,³ the free energy of interaction of the adsorbed molecules per unit area caused by the compression of adsorbed molecules can be expressed as follows:

$$E_R^{en} = N_s K T \theta_\infty \left(1 - \frac{d}{\delta} \right) \tag{3}$$

where d is the distance from the surface, δ is the thickness of adsorbed layer, and θ_∞ is 0.2.^{8,26} N_s is in general considered to be the number of segments adsorbed per unit area; here, however, the number of chains which may contribute to the steric hindrance for the approach of the particles, that is, the number of aliphatic chains, was used. The calculated number of aliphatic chains of polyamide A and B are 1.2×10^{14} and 1.3×10^{14} , respectively.

It should be noted here that the application of this equation is limited to the cases where surface coverage by the adsorbed molecules is sufficiently small to justify the neglect of their mutual interactions. The average surface areas of an aliphatic chain of polyamide adsorbed from cyclohexanone solution are shown in Table VII, which were calculated by dividing the surface area covered by one adsorbed polyamide molecule by the number of aliphatic chains in a molecule.

TABLE VII
Surface Area Occupied by Aliphatic Chain

Poly- amide	Adsorption, mg/g	Adsorption, mole/m ²	Surface area occupied by molecule, Å ²	Surface area occupied by aliphatic chain, Å ²
A	14	5.8×10^{-7}	290	73
B	25	2.1×10^{-6}	80	80
C	30	4.2×10^{-6}	42	42
D	32	5.7×10^{-6}	29	29
E	30	7.0×10^{-6}	24	24

Polyamide A and B give relatively large surface areas by comparison with the others, indicating that there is little interaction between their neighboring chains. Therefore, the entropic repulsion potential energies were calculated only for polyamide A and B. In calculating the potentials, there is some uncertainty about the correct value of the thickness of adsorbed layer. Since the thickness calculated from the viscosity measurements is that of a part of the polymer molecule which is fixed tightly to the surface, the thickness will be a little smaller than the actual thickness. It appears to be reasonable to use the values of 20 Å and 30 Å for the thickness of polyamide A and B, respectively. The total free energy of entropic repulsion was calculated from the product of eq. (3) and the contact areas of interacting

adsorbed layers. Assuming that the particles are spherical, the total free energy is given by the following equation:

$$E_R^{en} = \frac{N_s K T \theta_\infty \pi}{\delta} (\delta - d)^2 (2\gamma + \delta + d) \quad (4)$$

where γ is the radius of the particles. Although this calculation is based on the assumption that the adsorbed molecules are rigid, the maximum energy that chiefly governs the stability is equal for both rigid and flexible molecules.³

Effect of Zeta Potential on Dispersion

The electrical repulsion potential due to the electrical charge on the particle can be approximated by the following equation in nonaqueous systems:

$$E_R^{el} = \frac{\epsilon \gamma^2 \zeta^2}{R} \quad (5)$$

where R is the distance between the centers of the particles.

Zeta potentials for red iron oxide are shown in Table VIII. Electrostatic repulsion energies calculated for pure solvent, solution of polyamide A, and solution of polyamide B are $90(\gamma/R)KT$, $1.2(\gamma/R)KT$, and $27(\gamma/R)KT$, respectively. At normal temperatures, $KT = 4.1 \times 10^{-14}$ erg.

TABLE VIII
Zeta Potentials of Red Iron Oxide

Solvent	Polyamide	ζ -Potential, mV
Cyclohexanone	none	-60.0
	A	-22.0
	B	-33.2
	C	-40.9
	D	-43.8
	E	-20.4
Isopropyl alcohol	none	+61.5
	A	—
	B	—
	C	+30.0
	D	+15.0
	E	—

van der Waal's Energy of Attraction

The energy of attraction between two particles may be calculated according to the following formula derived by Hamaker²⁷:

$$E_A = -\frac{A}{6} \left(\frac{2}{S^2 - 4} + \frac{2}{S^2} + \ln \frac{S^2 - 4}{S^2} \right) \quad (6)$$

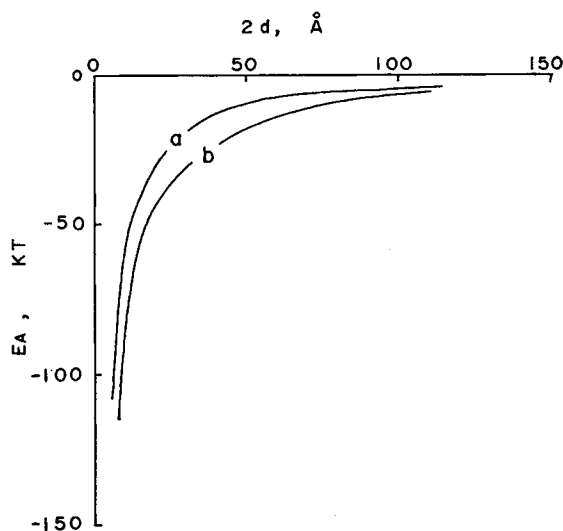


Fig. 7. van der Waal's attraction potentials between particles with adsorbed layer of 25-Å thickness (a) and without adsorbed layer (b).

where A is the Hamaker constant. The combined Hamaker constant in the system can be expressed as

$$A = A_{11} + A_{22} - 2A_{12} \tag{7}$$

where A_{11} is the Hamaker constant for the particles, A_{22} is that for the solvent, and A_{12} is the particle/solvent Hamaker constant. Referring to Crowl's data,²⁶ substituting 1.1×10^{-12} for A_{11} and 0.1×10^{-12} for A_{22} and approximating $A_{12} = \sqrt{A_{11}A_{22}}$, A is approximately equal to 10^{-12} . Vold⁵ developed an expression for E_A taking into account the presence of an adsorbed layer on the particle and including the Hamaker constant A_{33} for the material of the adsorbed layer.

The potential curve obtained from Hamaker's and Vold's equation for the particle containing an adsorbed layer 25 Å thick is shown in Figure 7, together with that containing no adsorbed layer. It can be seen that the presence of an adsorbed layer reduces the magnitude of the interaction potential.

Total Potential Energy

The potential energy curves for electrostatic repulsion, entropic repulsion, and van der Waal's attraction obtained in the preceding sections (dotted lines) and the combined total potential energy curves (solid lines) are plotted against the distance from the surface in Figure 8. The potential energy of red iron oxide containing no adsorbed layer was governed almost only by electrostatic repulsion, and the maximum was 33KT. If a 20-Å-thick layer of polyamide A is adsorbed, there is an energy barrier of steep slope; the

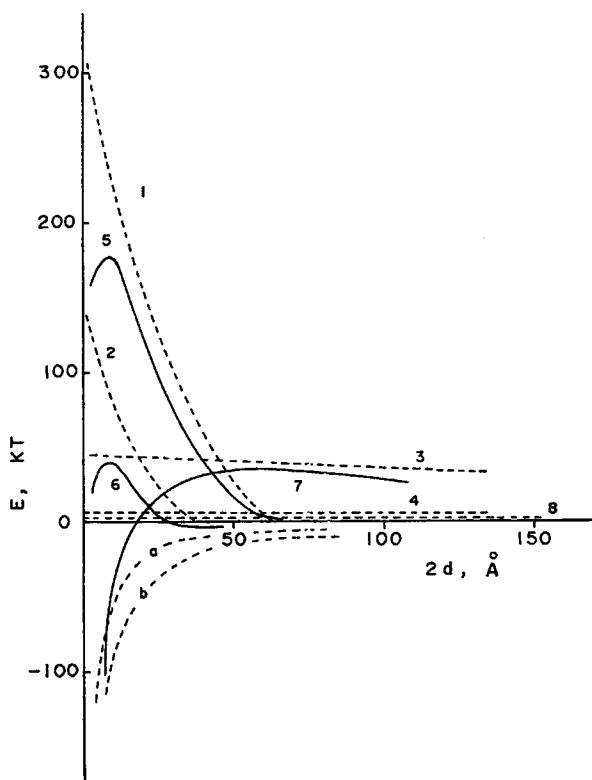


Fig. 8. Potentials between particles showing energy barriers: (1) entropic repulsion with adsorbed layer of polyamide B; (2) entropic repulsion with adsorbed layer of polyamide A; (3) electrical repulsion without adsorbed layer; (4) electrical repulsion with adsorbed layer of polyamide B; (5) total potential with adsorbed layer of polyamide B; (6) total potential with adsorbed layer of polyamide A; (7) total potential without adsorbed layer; (8) electrical repulsion with adsorbed layer of polyamide A.

maximum is $42KT$. If a $30\text{-}\text{\AA}$ -thick layer of polyamide B is adsorbed, the maximum energy reaches as high as $180KT$, indicating that the suspension is extremely stable, as verified by the sedimentation test.

It can be concluded from the foregoing that the dispersion stability of red iron oxide in polyamide solution is governed mainly by entropic repulsion of the adsorbed layer of polyamide. The effect of the adsorbed layer on the stabilization increases with the increase in the amount of adsorption, the thickness of the adsorbed layer, and the number of interacting segments in the polymer molecule.

Little contribution of electrostatic repulsion was observed in this system.

The author wishes to acknowledge Dr. Sugiura, Mr. Higuchi, Mr. Seto, and Mr. Shimizu of Central Research Laboratory of the Sony Corporation for their helpful suggestions in the course of this study and Dr. Shima, the president of Central Research Laboratory of Sony Corporation, for permitting the publication of this paper.

References

1. E. J. W. Verwey and J. Th. G. Overbeek, *Theory of the Stability of Lyophobic Colloids*, Elsevier, Amsterdam, 1948.
2. H. Koelmans and J. Th. G. Overbeek, *Discussions Faraday Soc.*, **18**, 52 (1954).
3. E. L. Mackor, *J. Colloid Sci.*, **6**, 492 (1951).
4. E. L. Mackor and J. H. van der Waals, *ibid.*, **7**, 535 (1952).
5. M. J. Vold, *ibid.*, **16**, 1 (1961).
6. E. J. Clayfield and E. C. Lumb, *J. Colloid Interfac. Sci.*, **22**, 269 (1966).
7. E. J. Clayfield and E. C. Lumb, *ibid.*, **22**, 285 (1966).
8. A. L. Romo, *J. Phys. Chem.*, **67**, 386 (1963).
9. W. Heller and T. L. Puch, *J. Polym. Sci.*, **47**, 203 (1960).
10. Y. Yamashita and O. Morita, *Shikizai Kyokaiishi*, **42**, 399 (1969).
11. R. H. Shiesser, Ph.D. Thesis, Lehigh University, 1966.
12. R. H. Shiesser, W. D. Schaeffer, and A. C. Zettlemyer, *J. Oil Colour Chem. Ass.*, **50**, 865 (1967).
13. H. Wittcoff, Conference, Tokyo, Sept. 1969.
14. A. Kitahara, H. Yamada, Y. Kobayashi, H. Ikeda, and M. Koshinuma, *Kogyo Kagaku Zasshi*, **70**, 2222 (1967).
15. E. Guth and O. Gold, *Phys. Rev.*, **53**, 322 (1938).
16. E. C. Rothstein, *Official Digest*, **36**, 1448 (1964).
17. A. Doroszkowski and L. Lambourne, *J. Colloid Interfac. Sci.*, **26**, 214 (1968).
18. F. Rowland, R. Bulas, E. Rothstein, and F. R. Eirich, *Ind. Eng. Chem.*, **57**, 46 (1965).
19. R. Perkel and R. Ullman, *J. Polym. Sci.*, **54**, 127 (1961).
20. S. Ellerstein and R. Ullman, *ibid.*, **55**, 123 (1961).
21. G. J. Howard and P. McConnell, *J. Phys. Chem.*, **71**, 2974 (1967).
22. G. J. Howard and P. McConnell, *ibid.*, **71**, 2981 (1967).
23. G. J. Howard and McConnell, *ibid.*, **71**, 2991 (1967).
24. G. Steinberg, *ibid.*, **71**, 292 (1967).
25. T. Sato, T. Tanaka, and T. Yoshida, *J. Polym. Sci. B*, **5**, 947 (1967).
26. V. T. Crowl, *J. Oil Colour Chem. Ass.*, **50**, 1023 (1967).
27. H. C. Hamaker, *Physica*, **4**, 1058 (1937).

Received November 5, 1970

Revised February 2, 1971